International Journal of Applied Engineering Research ISSN 0973-4562 Volume 13, Number 8 (2018) pp. 6332-6339

Design and Simulation of the High Sensitivity Detection of Hemoglobin (Hb) Concentration in Human Blood by The Core-shell Enhanced Surface Plasmon Resonance (SPR)-Based Biosensor

Widayanti[1,2], Kamsul Abraha[2], Agung Bambang Setio Utomo[2]

[1]Departement of Physics, Faculty of Science and Technology, Sunan Kalijaga Islamic State University, Jl. Marsda Adi Sucipto No.1 Yogyakarta, Indonesia.

[2]Departement of Physics, Faculty of Mathematics and Natural Sciences, Gadjah Mada University, Jl. Sekip Utara BLS.21 Yogyakarta, Indonesia.

Abstract

In this paper, we present the design and simulation of the detection amplification technique through *Attenuated Total Reflection* (ATR) spectrum based on the core-shell enhanced Surface Plasmon Resonance (SPR) in the Kretschmann configuration. The system consists five-layer materials, i.e prism/Ag/core-shell/PEG/Hemoglobin (Hb). The biosensor performance can be seen from the reflectivity spectra for the configuration of SPR-based biosensor presented and depends on the dielectric function and thickness of each layer material. Core-shell is the nanocomposite spherical nanoparticle consisting of a spherical Fe_3O_4 as the core covered by Au shell (Fe_3O_4@Au core-shell) used as an active material for Hb concentration detection in the wavelength 632.8 nm. Effective permittivity determination of the core-shell nanoparticle (Fe_3O_4@Au) is done by applying the *Effective Medium Theory* (EMT) approximation and the calculation of the reflectivity is carried out by varying the size *(r)* and volume fraction *(F)* of the core-shell. In this simulation, two prisms, i.e BK7 and chalcogenide (2S2G) are used and the reflectivity spectra for both prisms are investigated, in which the Ag thin film is used as the metal layer mounted on top of the prism. The refractive index of the core-shell is varied depending on the *r* and *F* of the core-shell. The performance of this presented model of SPR system is shown at reflectivity spectrum, and calibration curve. Our results show that by varying the radius of the core (*r*), the shell thickness, and the *F* of the core-shell, the dip of the reflectivity (ATR) spectrum is shifted to the larger angle of incident light and the involvement of the core-shell in the SPR-based biosensor leads to enhancement of the SPR biosensor performance for Hb concentration detection. For BK7/Ag/core-shell/PEG/Hb, at r = 2.5 nm, F = 0.27 and the Hb concentration 20 g/L, the simulation results that the sensitivity value for core-shell involvement configuration ($0.021^0/gL^{-1}$) is greater than that with no core-shell involvement ($0.018^0/gL^{-1}$). The resolution of Hb concentration detection is 0.0476 g/L, and the sensitivity increas by 16.6 % compared to the sensitivity of the conventional SPR-based biosensor without core-shell addition.

Keyword: Surface Plasmon Resonance, Core-shell Fe_3O_4@Au, Reflectivity

INTRODUCTION

Surface plasmon resonance (SPR) spectroscopy is an optical spectroscopy for quantitive analysis of the interaction between the metal film surface and the dielectric material mounted on top of the metal. SPR sensor is very sensitive to a slight change in the refractive index of the dielectric or material in the near vicinity of the thin metal surface. Hence, the SPR sensing techniques have been widely used in many different areas and are applied extensively as sensors for monitoring specific interaction between antigen-antibody, reseptor-ligand, etc based on the affinity activity (chemical reaction). These molecular interactions can be monitored in real-time, label free and rapid sensing capability [1]. The first application of the SPR sensing is the gas sensing [2] and after that, several research works have been carried out in the topic of SPR sensors by experimental and theoretical approximations. Biomolecular interaction sensing was initially reported by Nylander and Liedberg in 1982 [3]. They used a system with organic layer that reversibly absorbs the anaesthetic gas halothane. More potential applications and new devices have been used and reported. Among of them are the detection of DNA hybridization [4], acetylcholinesterase [5], membrane protein [6], and human blood-group [7].

The SPR phenomenon emerges from the existence of a plasmon wave, an induced effect of the coupling between electromagnetic field (*p*-polarized) with the plasma oscillation [8,9]. Coupling occurs when the wave vector of the evanescent wave (EW) matches the wave vector of the surface plasmon (SP) under the total internal reflection condition expressed as equation (1)

$$k_0 n_p \sin\theta_{SPR} = k_0 \left(\frac{\varepsilon_m n_d^2}{\varepsilon_m + n_d^2}\right)^{\frac{1}{2}} \quad ; \; k_0 = \frac{2\pi}{\lambda}$$

$$\theta_{SPR} = sin^{-1}\left(\frac{\varepsilon_m n_d^2}{(\varepsilon_m + n_d^2){n_p}^2}\right)^{\frac{1}{2}} \qquad (1)$$

where k_0 is the propagation constant of an incident light beam (of wavelength λ) in the vacuum. The term on left hand side is the wave vector of evanescent wave (K_{EW}) incident at a resonance angle θ_{SPR} through the light coupling device (prism) of refractive index n_p. The right hand side term is the wave vector (K_{SP}) of surface plasmon (SP) with ε_m is the real part

of the metal permittivity and n_d as the refractive index of dielectric material or sensing medium.

The wave vector of the SP wave is a function of refractive indices of the dielectric, metal and analyte i.e the sensing medium. If there is a local change in the refractive index of the sensing medium near the metal surface, it will in turn lead to a change in the propagation constant of SP as well as in the angle of incidence light in order to satisfy the resonance. A sharp dip of reflected output shows this resonance due to strong absorbtion by SP wave.

Generally, the SPR biosensor is set up in the Kretschmann's configuration in which a thin metallic film is deposited on a prism and the dielectric medium or biology element to be sensed is mounted on top [10]. In this configuration a light wave is totally reflected at the interface between a prism coupler and a thin metal layer and excites an SP at the outer boundary of the metal by evanescently tunneling through the thin metal layer. Whereas, the metallic layer that is used in SPR biosensor measurement consists of either gold or silver.

Although SPR biosensor has the advantage of rapid and direct sensing and surface plasmon used in SPR spectroscopy is highly sensitive to changes in the surrounding refractive index, but for detecting low molecular weight e.g low concentration of analyte (proteins) [11], DNA, or bacteria [12], the change in SPR response is very limited and constrained by the poor attachment of biomolecule on the metal surface [13]. This is due to the very small changes of the refractive index [14] under a metal layer. Consequently, several methods had been applied to increase the SPR sensitivity and performance for detecting low molecular weight of biomolecules. Among them, metal nanoparticles were introduced due to their properties which support localized SPR (LSPR) on particle surface and on the coupling between nanoparticle SP and bulk SP on the Au thin film. Nanotechnology offers a broad range of potential applications to biology system, optical communication and new material detection [15].

Currently, the development of the new material that combines multiple functions or properties had attracted considerable attention because of its revolutionary technology for sensitivity enhancement of surface plasmon resonance (SPR)-based biosensor. Those materials are the magnetic and plasmonic nanoparticles as the active materials for biomolecule detection [11,16]. One of the magnetic and plasmonic materials is the nanoparticle core-shell. Some studies have observed that the optical response or resonance spectrum of the core-shell depends on the thickness of the shell, the size of the core and the volume fraction (F). One of the core-shell is Fe_3O_4@Au. The presence of Fe_3O_4@Au is capable to enhance the immobilization of biomolecules e.g the DNA of chum salmon [17], antibody IgG [18], Haemoglobin [19],] thrombin [20], and protein concentration of interleukin IL17 [21]. Corresponding with the core-shell properties, the coating of Au shell for the magnetic core protected it from oxidation and aggregation. Therefore the stabilization of the core-shell (Fe_3O_4@Au) was enhanced *obviously*. Corresponding with the biomolecules have been detected with SPR-based biosensor, the detection of the Hb concentration have been explored by SPR-based biosensor for three wavelengths (401.5 nm, 589.3 nm and 706.5 nm) with haemoglobin concentration varying between 0 and 140 g/l [7].

This paper focuses on the simulation of the core-shell effective permittivity calculation that depends on the volume fraction and the size of the core-shell. Furthermore, SPR-based biosensor reflectivity for Hb concentration in human blood detection with the core-shell involvement is investigated. Finally, the performance improvement of the SPR-based biosensor for Hb concentration detection i.e the sensitivity, resolution of measurement, and the sensitivity enhancement is estimated.

MATERIALS AND METHOD

In this section, we discuss elements of the proposed SPR-based biosensor design and setup.

A. Multilayer SPR-based biosensor configuration

In this study, we apply the design consideration for SPR-based Hb concentration detection. We use the Kretschmann configuration[10] with five layers i.e prism/Ag/core-shell/PEG/Hb as shown in Fig.1 And then, we determine the effective permittivity of the core-shell and calculate reflectivity in the Attenuated Total Reflection (ATR) method by analytical and computational approximation. The angle ϕ_i and ϕ_r are the incident and the reflection angle respectively, d_1 is the thickness of metal layer, d_2 is the thickness of core-shell and k_x is the wave vector component along x-axis.

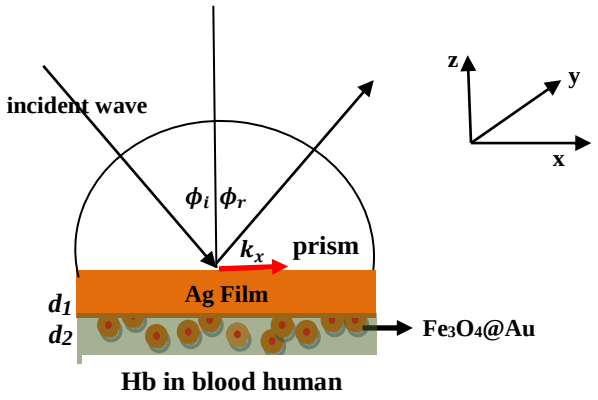

Figure 1: Kretschmann geometry of ATR methods in SPR-based biosensor with the involvement of Fe_3O_4@Au core-shell

When the resonance happens, any change in refractive index near the metal-dielectric interface (change of the Hb concentration) causes a shift in the resonance (SPR curve). The Fe_3O_4@Au core-shell is performed using the model as shown in Fig 2. The magnetic nanoparticle core-shell consists of a Fe_3O_4 core of radii b coated by a metallic Au of thickness $(a-b)$. The dielectric constants of the magnetic nanoparticle and the metallic Au are ε_c and ε_s , respectively

.

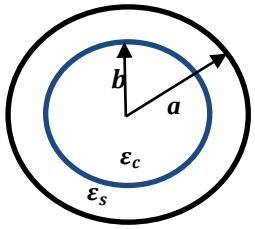

Figure 2: The core-shell geometry model contains Fe_3O_4 (core) and Au (shell). Fe_3O_4 has radius b and permittivity ε_c, the total nanoparticle radii is a and permittivity is ε_s.

The present work in this SPR configuration reports the design by making use of the experimental data of Hb concentration from Zhernovaya et.al [22]. The dielectric constant of Hb is varied from 1.338 to 1.340. Through reflectivity measurement and Kramers-Kronig analysis, the value of complex ε_c is obtained (Schlegel, et al) [23] and ε_s can be quoted from Johnson and Christy work [24] and then from the internal homogenization for plasmonic and dielectric constituent materials, the effective permittivity (ε_{eff}) of Fe_3O_4@Au core-shell is *derived* [25] , which gives the result

$$\varepsilon_{\text{eff}} = \varepsilon_s \frac{a^3(\varepsilon_c + 2\varepsilon_s) + 2b^3(\varepsilon_c - \varepsilon_s)}{a^3(\varepsilon_c + 2\varepsilon_s) - b^3(\varepsilon_c - \varepsilon_s)} \qquad (2)$$

The refractive index of the BK7 glass prism is 1.510, and the 2S2G prism is 2,327 in the wavelength of the electromagnetic wave 632.8 nm, and the complex refractive index of silver is 0.13455+3.98651i [24]. The thickness of Ag film is d_l=40 nm. In this simulation, the size or radius of the core-shell (r) is varied from 2,5 to 7.5 nm and volume fraction (F) is varied from 0.27 to 0.85. The ATR reflectivity R is given by the Fresnel equation [26].

$$R = \left|r_{ijk}\right|^2 = \left|\frac{r_{ij} + r_{jk}e^{2ik_{jz}d_j}}{1 + r_{ij}r_{jk}e^{2ik_{jz}d_j}}\right|^2 \qquad (3)$$

with

$$r_{ij} = \frac{k_i\varepsilon_j - k_j\varepsilon_i}{k_i\varepsilon_j + k_j\varepsilon_i} \qquad (4)$$

where r_{ij} is the surface reflectivity coefficient between medium i and medium j. k_{ij} is the wave vector component perpendicular to the surface, k_x is the wave vector component parallel to the surface as shown in Fig.1, whereas d_j and ε_i are respectively the j-th layer thickness and the i-th medium dielectric constant.

B. Light Coupling Prism

The light coupling prism BK7 and calchogenide (2S2G) have wavelength dependent refractive indices that are represented by the expression as follows [7]

$$n_c(\lambda) = \sqrt{1 + \frac{A_1\lambda^2}{\lambda^2 - B_1^2} + \frac{A_2\lambda^2}{\lambda^2 - B_2^2} + \frac{A_3\lambda^2}{\lambda^2 - B_3^2}} \qquad (5)$$

where λ denotes the wavelength in μm and the coefficients A_1, A_2, A_3, B_1, B and B_3 are known as Sellmier coefficients and have numeric values for BK7 prism [27] and for 2S2G prism [28]. These numeric values are determined experimentally by measuring spectral variation in a material.

C. Metal Layer

The prism has been coated with a thin metal film (Ag of thickness 40 nm). Ag is chosen as SPR active metal due to its narrow absorbance resonance spectrum among the other metals. From the free-electron Drude model, the wavelength-dependent complex permittivity of Ag metal can be written as [7]

$$\varepsilon_m = \varepsilon_{mr} + i\varepsilon_{mi} = 1 - \frac{\lambda^2\lambda_C}{\lambda_p^2(\lambda_C + i\lambda)} \qquad (6)$$

where λ_p is the plasma wavelength and λ_c is the collision wavelength for Ag.

D. Fe_3O_4@Au core-shell

Magnetic nanoparticle Fe_3O_4 (magnetite) for the core and gold for shell in the coreshell are beneficial for nanoscale sensing. Fe_3O_4 has a large surface to volume rasio and possesses high surface energies, therefore they tend to aggregate for minimize the surface energies. Based on these properties, it is important to keep the stability of nanoparticle magnetite with the protection strategies comprising coating with metal material. In many cases the protecting shell (Au metal) stabilizes the magnetite nanoparticle and it is used for further functionalization [29].

E. Buffer Layer

The Ag layer in SPR-based biosensor must be followed by a buffer layer in the vicinity of 1-15 nm in order to achieve highly sensitive sensor [30]. This buffer is the biochemical layer because it must prevent the analyte (Hb) from being in direct contact with Au layer (shell of Fe_3O_4@Au) and its structural compatibility with analyte (Hb) *Poly ethylene glyco*l (PEG) is chosen as the buffer material thst can satisfy the above conditions. PEG for this study is assumed to be in10 nm.

F. Hb in human Blood as analyte layer

Blood sample in which Hb is included with certain concentration is chosen as sample or analyte layer, the topmost layer in the SPR biosensor. From the data of Zhernovaya et.al [22] and Prahl [31], the complex refractive index of Hb concentration that is wavelength dependent can be described as

$$n_s = n + ik \qquad (7)$$

Here n is the real part and k is the imaginary part of the complex refractive index of Hb concentration. n is found to be much greater than k. The thickness of Hb is limitless

because there is no change from the calculation that is carried out, namely from 1nm to 1 μm [7]. The normal Hb concentration is defined for different age-group. Its range is 100-135 g/L for children, 130-170 g/L for adult male and 120-155 g/L for adult female. The real part of Hb refractive index has been measured for different concentration and visible wavelength [22] in the form of Barer's expression (Barer) given as

$$n = n_0 + \alpha C_H \qquad (8)$$

where n_0 is the effective refractive index of blood sample at zero Hb concentration, α is the specific refraction increment and C_H is the Hb concentration. The data using in this study is based on the above experimental result.

G. SPR Biosensor performance from ATR spectrum

The indicator of sensor's performance in this simulation can be obtained from reflectivity spectrum (sensitivity and sensitivity enhancement), calibration curve (ϕ_{SPR} vs C_H) and the resolution.

The sensitivity of SPR-based biosensor is written as [32]

$$S = \frac{\Delta\theta_{\mathrm{SPR}}}{\Delta n} = \frac{\theta_{\mathrm{SPR}}(\varepsilon_d + \Delta\varepsilon_d) - \theta_{\mathrm{SPR}}(\varepsilon_d)}{\Delta n} \qquad (9)$$

where $\Delta\theta_{SPR}$ is the difference of the SPR angle and $\Delta n = \Delta C_H$ is the change in refractive index.

RESULT AND DISCUSSION

Acoording to the equation (5), in the 632.8 nm wavelength, 2S2G prism have greater refractive index (2.37) than BK7 prism (1.5151). Therefore from the equation (1), we get greater θ_{SPR} for BK7 (43.35^0) than for 2S2G prism (26.52^0) as shown in Fig 3 for prism/Ag/air configuration.

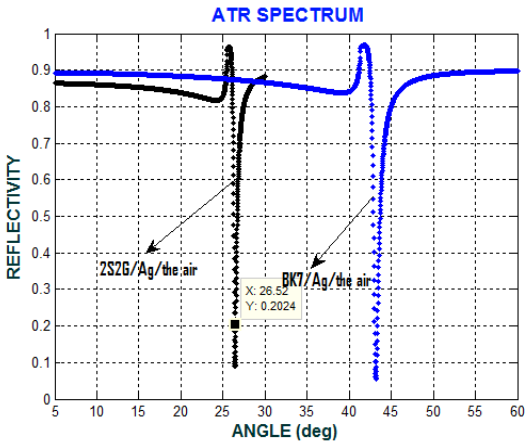

Figure 3: The ATR spectrum for Prism/Ag/air configuration

Three layer system above is the conventional SPR before analyte sensing. θ_{SPR} will change if we add the other material on top metal thin film (Ag). Here, for detection of Hb concentration in blood human, we use the formation of the four layers (Prism/Ag/PEG/Hb) without the core-shell and of the five layers (Prism/Ag/ Fe_3O_4@Au/PEG/Hb). We then determine the ATR spectrum (reflectivity) and calculate the parameters of performance. The change of θ_{SPR} depends on the refractive index or permittivity and thickness of each layer material. From the results, we investigate the SPR phenomenon for four layer and five layer configurations.

For the layer in which the core-shell is involved, its effective permittivity varies depending on the size of the core, the thickness of the shell and the volume fraction of the core-shell as shown at Table 1. Therefore, if the core-shell is applied to SPR-based biosensor system, its effective permittivities change leads to the shift of SPR angle to the right or to the larger angle of incidence. It is shown that there is sensitivity enhancement of biosensor.

Table 1: The varied effective permittivity of the core-shell

Core radii b (nm)	*Core-shell radii a* (nm)	*shell thickness (a-b)* nm	*volume fraction (F)*	*effective permittivity of core-shell (ε_{ff}) real part , imaginary part*
7.125	7.5	0.375		
4.75	5	0.250	0.85	1.9626 , 5.0803
2.375	2.5	0.125		
6.375	7.5	1.125		
4.25	5	0.750	0.61	-0.7091 , 4.8433
2.125	2.5	0.375		
5.25	7.5	2.250		
3.75	5	1.250	0.42	-3.2664 , 4.3465
1.75	2.5	0.750		
4.875	7.5	2.625		
3.25	5	1.750	0.27	-5.5378 , 3.6706
1.625	2.5	0.875		

SPR is very sensitive to the change of refractive index and thickness on the surface. The thicknes of Ag metal is one of the parameters that must be controlled in order to obtain an optimum performance of SPR biosensor. In this study by varying the Ag thickness from 20 to 60 nm, the most desirable resonance peak of Ag metal film thickness is obtained at 40 nm.

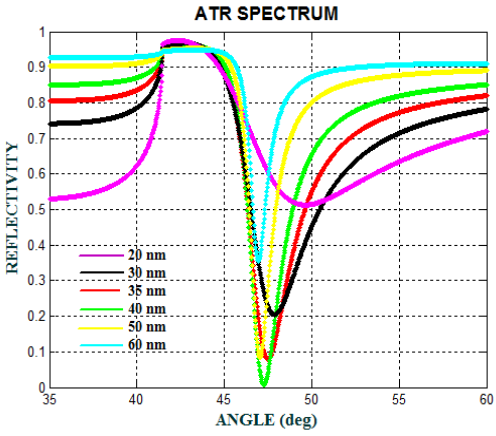

Figure 4: The ATR spectra for the Ag metal thickness varied from 20 nm to the 60 nm.

When Ag thin film is very thin (20-30 nm), there is more coupling into the SP mode but due to light scattering, the sensitivity is reduced, whereas at 50-60 nm, the depth of the resonance peak decreases indicating the reduced coupling efficiency of light with the SP mode on the film. This means that the metal begins acting as a reflectance plane when its thickness increases to a point where light cannot couple into the surface charge oscillations that make up the plasmon mode. Fig 4 shows the optimal thickness to support SPR system determined to lie at 40 nm.

Occurence of SPR based biosensor with the present haemoglobin (Hb) detection shceme can be seen from the reflectivity spectrum. The configuration consisting of nanoparticle core-shell is shown in Fig 5 (a) for BK7 Prism and Fig 5 (b) for 2S2G prism.

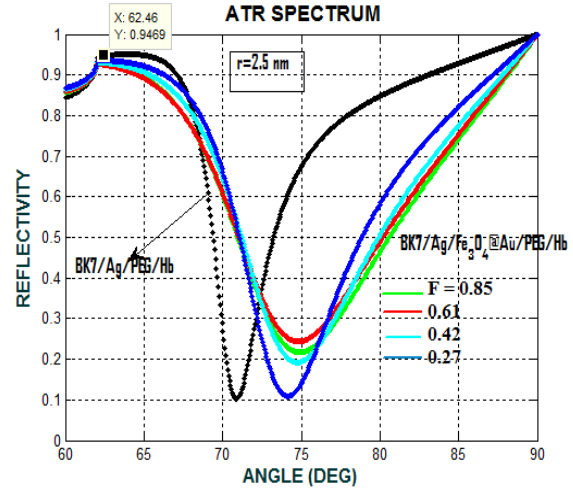

(a)

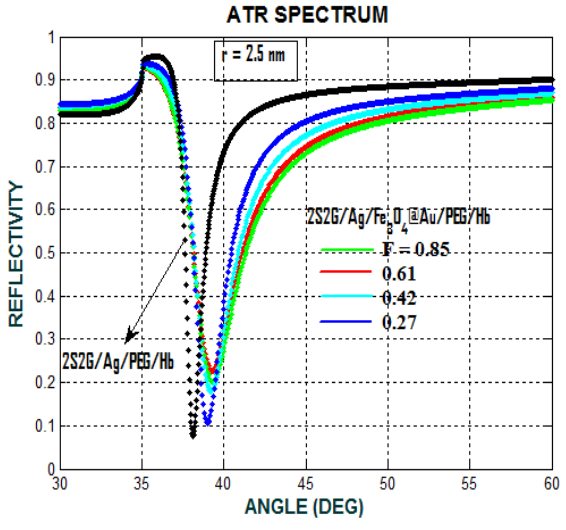

(b)

Figure 5: The ATR spectra with the radii of the core-shell *r*=2.5 nm for the (a) BK7 prism and (b) 2S2G prism. The F of core-shell varies from 0.27 to the 0.85 with Hb concentration of 20 g/L.

Here, for Hb concentration detection we chose the value of Ag thickness is 40 nm, the radii of the core-shell was varied at 2.5 nm, 5 nm, and 7.5, the volume fraction was varied at 0.27, 0.42, 0.61, and 0.85. For BK7 prism, the dip of the ATR curve occurs at the incident angle 71.40° (*black line*) for SPR system configuration only consisting of three layers (Prism/Ag/PEG/ Hb). And then, the dip of the reflectivity curve is shifted to the larger incident angle after the Fe_3O_4@Au core-shell has been deposited onto the surface of the Ag thin film. Referring to Fig 5 (a) for the radius of 2.5 nm and the Fe_3O_4@Au volume fraction (F) varied at 0.27, 0.42, 0.61 and 0.85, the SPR angle is shifted to the larger angle at 74.16^0;74.75^0; 74.80^0; and 74.82^0. By increasing the volume fraction (F), the angle of resonance increases as well. It can be seen in Fig 5 (a) that the minimum reflectivity is seen at 74.16° for F=0.27. Similar to that, Fig 5 (b) for the 2S2G prism shows that the SPR angle is shifted to the larger angle as well. For the other core-shell radii, they are shown in Fig 6 (a) and Fig 7 (a) for the BK7 prism and in fig 6 (b) and Fig 7 (b) for the 2S2G prism.

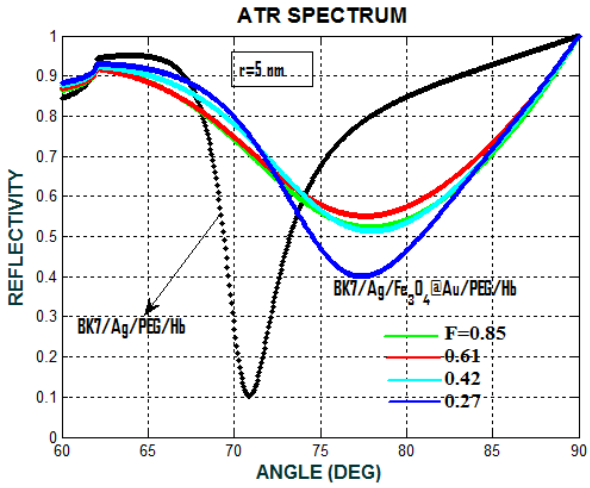

(a)

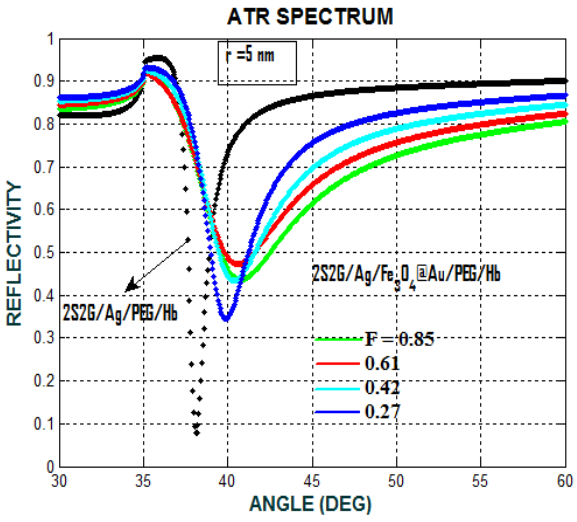

(b)

Figure 6: The ATR spectra with the size (radii) of the core-shell *r*= 5nm for the (a) BK7 prism and (b) 2S2G prism. The F of the core-shell varies from 0.27 to the 0.85 with Hb concentration of 20 g/L.

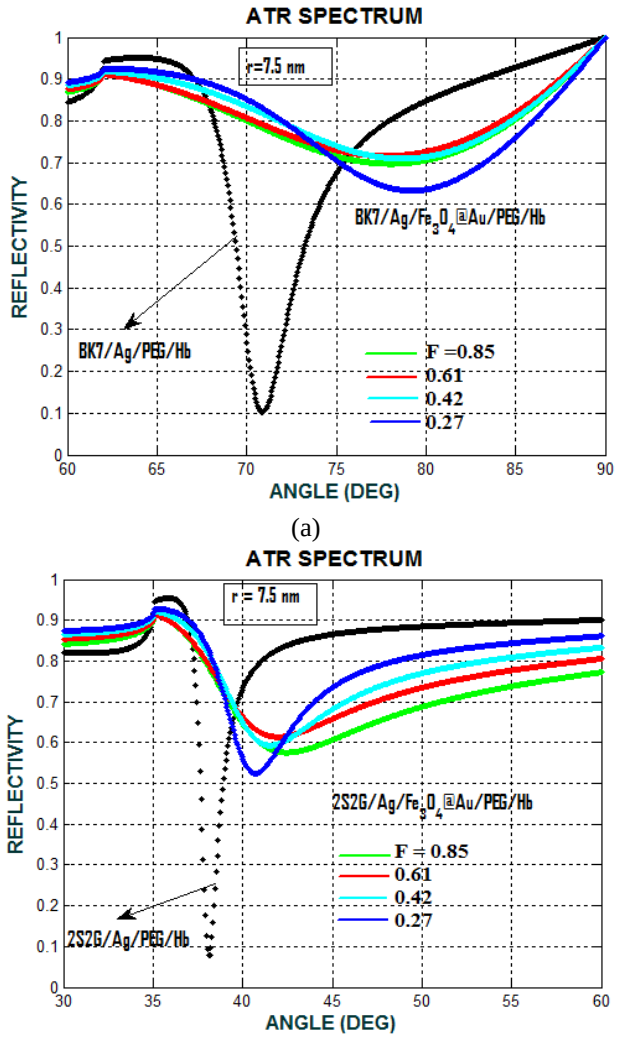

Figure 7: The ATR spectra with the size of the core-shell *r*= 7.5nm for the (a) BK7 prism and (b) 2S2G prism. The F of the core-shell varies from 0.27 to the 0.85 with Hb concentration of 20 g/L

Based on the above results, we can choose the values of the core radius, the shell thickness and or the volume fraction *F* for yielding the desirable effective permittivity of the Fe_3O_4@Au core-shell giving optimum performance of SPR based biosensor for Hb concentration detection. From those results, we choose the radius core-shell is 2.5 nm, the volume fraction is 0.27, and the prism is BK7. The Hb concentration is varied from 20 g/L, 60 g/L, 100 g/L, and 140 g/L. Fig 8 (a) shows the ATR spectra for varied Hb concentration detection for prism/Ag/PEG/Hb configuration. For four Hb concentration values, i.e. 20 g/L, 60 g/L, 100 g/L, and 140 g/L, θ_{SPR} shifts to 70.92^0, 71.52^0, 72.3^0, and 73.08^0. Whereas, Fig 8 (b) is for prism/Ag/Fe_3O_4@Au/PEG/Hb configuration, and θ_{SPR} shifts to 74.22^0, 75.00^0, 75.84^0, and 76.86^0 .

Following the reflectivity spectrum (ATR spectrum) and the θ_{SPR} obtained from the simulation of the SPR-based biosensor with five layer configuration (BK7/Ag/Fe_3O_4@Au/PEG/Hb), we can then determine some parameters which characterize the biosensor performance, e.g calibration, sensitivity, resolution and sensitivity enhancement.

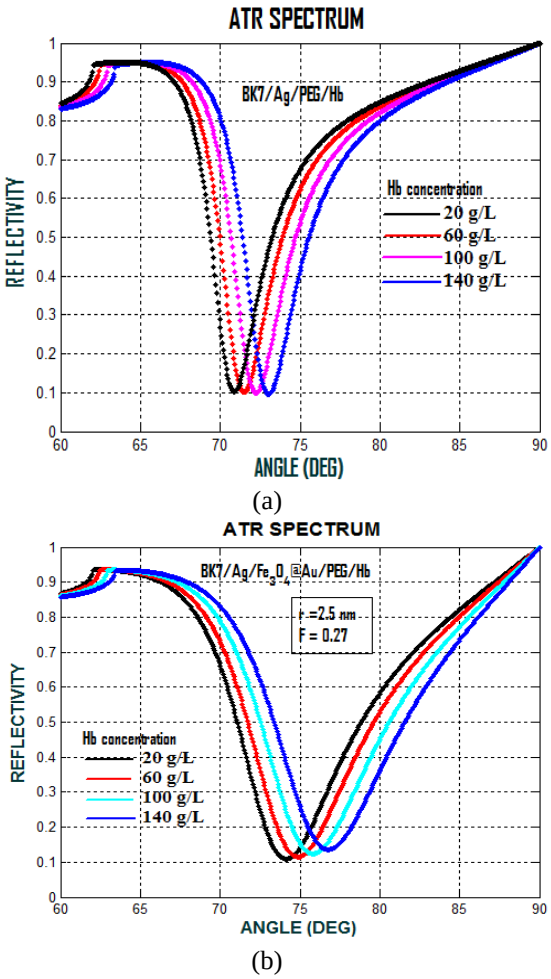

Figure 8: ATR Spectra for Hb concentration variation: (a) Prisma/Ag/PEG/Hb configuration (b) Prisma/Ag/core-shell/PEG/Hb

The calibration of measurement is obtained from the calculation of the θ_{SPR} and Hb concentration C_H. Fig 9 shows a positive calibration curve, indicating that as the Hb concentration increases, the SPR curve should shift to a greater value of θ_{SPR}.

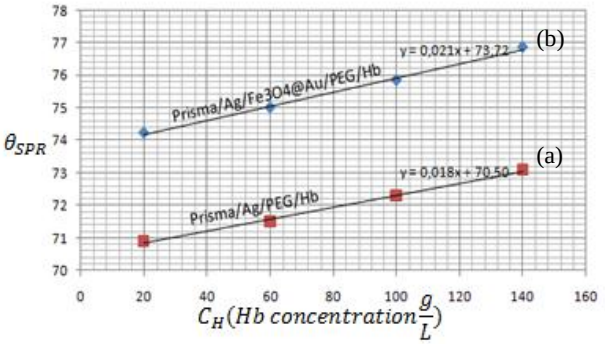

Figure 9: Calibration curve for (a) four layers and (b) five layers configuration

The above θ_{SPR} values are separated from one another in a linear fashion exhibiting an overall angle shift of 4.16^0 (no core-shell) and 2.64^0 (with core-shell) for a corresponding variation 20 to 140 g/L in Hb concentration. The slope of calibration curve $\left({}^{\delta\theta_{SPR}}/_{\delta C_H}\right)$ represents the sensitivity of Hb concentration detection (as mentioned in equation 9). The sensitivity value for core-shell involvement configuration ($0.021^0/gL^{-1}$) is greater than that with no core-shell involvement ($0.018^0/gL^{-1}$). Furthermore, if the angle resolution of 0.001^0, is taking into account, the resolution of Hb concentration detection (ΔC_H) in this study is 0.0476 g/L.

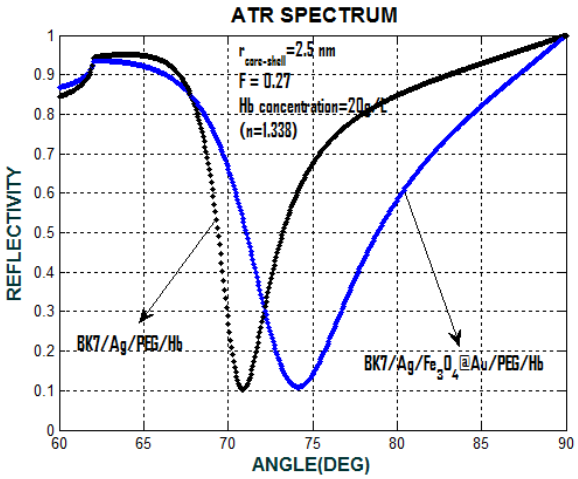

Figure 10: ATR spectra for (BK7/Ag/PEG/Hb) and (BK7/Ag/core-shell/PEG/Hb)

Sensitivity enhancement for this presented research can be seen from the ATR curves in Fig 10. Therefore, it can be obtained that for the core-shell radius 2.5 nm, the sensitivity increased by 16.6 % for *F*=0.27, compared to the sensitivity of the conventional SPR-based biosensor without core-shell addition.

CONCLUSIONS

In summary, we have presented a simulation of a SPR-based biosensor for accurate detection of Hb concentration in human blood. The result indicates that the property of the magnetic plasmonic materials leads to the improvement of the SPR-based biosensor performance i.e the sensitivity, resolution and sensitivity enhancement. By varying the radii of the core (*r*) and the shell (Au), and the volume fraction (*F*), the refractive index or the effective permittivity of the core-shell changes. The change in this effective permittivity results in the change of the dip position in that the SPR angle shifts to the right in the reflectivity spectrum. This *large shift* in the *dip* angle suggests the potential for its application in the highly sensitive biosensor, in this case, for sensing Hb concentration in human blood.

REFERENCES

[1] Homola, J., 2003, "Present and future of surface plasmon resonance biosensors," *Anal. Bioanal. Chem*., 377, pp.528-539.

[2] R.C. Jorgenson, R. C., Yee, S. S., 1993, "A fiber-optic chemical sensor based on surface plasmon resonance, "*Sensors and Actuators* B 12., pp 213–220.

[3] Liedberg, B., Nylander, C., and Lundstrom, I., 1983, "Surface plasmons resonance for gas detection and biosensing, "*Sens.Actuators* vol 4**,** pp. 299–304.

[4] He, L., Musick, M. D., Nicewarner, S. R., Sallinas, F.G., Benkovic, S. J., Natan, M. J., Keating, C. D., 2000,"Colloidal Au-Enhanced SPR for ultrasensitive Detection of DNA Hybridization*," Journal Am.Chem Soc* 122, pp 9071-9077.

[5] Milkani, E., Lambert, C. R., McGimpsey, W. G., 2011, "Direct detection of acetylcholinesterase inhibitor binding with an enzyme-based surface plasmon resonance sensor, "*Anal. Biochemistry,* 408 pp 212-219.

[6] Salamon, Z., Macleod, H.A., and Tollin, G., 1997, *Biochim. Biophys. Acta* 1331, pp 131-152.

[7] Sharma, A. K., 2013, "Plasmonic biosensor for detection of hemoglobin concentration in human blood: Design considerations," *J. Appl. Phys*. 114, 044701 10.1063/1.4816272.

[8] Homola, J., Yee, S. S., Gauglitz, G., 1993, "Surface plasmon resonance sensor: review, "*Sens.Actuators B* 54, pp 3–15.

[9] Maier, S. A., 2007, "*Fundamentals and Applications",* Plasmonics, Springer.

[10] Kretschmann, E., and Raether, H., 1968, "Radiative Decay of Non-Radiative Surface Plasmons Excited by Light," *Zeitschrift Naturforsh* 23 A, pp 2135-2136.

[11] Liang, R., Yao, G., Fan, L., Qiu, J., 2012, "Magnetite Fe_3O_4@Au composite–enhanced surface plasmon resonance for ultrasensitive detection of magnetit nanoparticle enriched α-fetoprotein," *Analytica Chimica Acta* 737, pp 22-28.

[12] Wu, L., Chu, H. S., Koh, W. S., and Li, E. P., 2010, "Highly Sensitive Graphene Biosensors base on Surface Plasmon Resonance, *Optics Express, "*vol. 18**,** pp. 1314.

[13] Rai, P., Mallidi, S., Zheng, X., Rahmanzadeh, R., Mir, Y, Elrington, S., 2010, "Development and applications of photo-triggered theranostic agent,", *Adv Drug Delivery Rev,* pp 621094-124.

[14] Wang, J., Sun, Y., Wang, L., Zhu, X., Zhang, H.,. Song, D., 2010, "Surface plasmon resonance biosensor based on Fe_3O_4/Au nanocomposites," *Colloid and Surfaces B: Biointerfaces* 81**,** pp 600-606.

[15] Eustis, S., El Sayed, M. A., 2006, "Why gold nanoparticles are more precious than pretty gold: noble metal surface plasmon resonance and its enhancement of the radiative properties of nanocrystals of different shapes, " *Chemical Society Reviews* 35, pp 209-217.

[16] Frasconi,M., Tortolini, C., Botre, F., Mazzei, F., 2010, *Anal. Chem*, Vol .82, pp. 77335-7342.

[17] Zhou, h., Lee, j., Park, T., Lee, S., Park, J., and Lee, J., 2012, "Ultrasensitive DNA Monitoring by Au-Fe_3O_4 Nanocomplex, "*Sensors and Actuator B: Chemical,* vol. 163, pp. 224-232.

[18] Wang, J., Song, D., Zhang, H., Zhang, J., Zhou, H., and Sun, Y., 2013, "Studies of Fe_3O_4/Ag/Au Composites for Immunoassay based on Surface Plasmon Resonance Biosensor, "*Colloids and Surfaces B: Biointerfaces*, vol. 102, pp. 165-170.

[19] Liu, Y., Han, T., Chen, C., Bao, N.,Yu, C., and Gu, H., 2011, "A novel Platform of hemoglobin on coreshell Structurally Fe3O4@Au Nanoparticles and its direct Electrochemistry, "*Electrochimica Acta,* vol. 56, pp. 3238-3247.

[20] Chen, H., Qi, F., Zhou, H., Jia, S., Gao, Y., Koh, K.,, and Yin, Y., 2015, 'Fe_3O_4@Au Nanoparticles as a means of Signal Enhancement in Surface Plasmon Resonance Spectroscopy for thrombin Detection," *Sensor and Actuator B: chemical,* vol. 212, pp. 505-511.

[21] Guo, x., 2014, "Fe3O4@Au nanoparticles enhanced surface plasmon resonance for ultrasensitive immunoassay," *Sensor and Actuator*, vol. 205, pp. 276-280.

[22] Zhernovaya, O., Sydoruk, O., Tuchin, V., and Douplik A, 2011, "The refractive index of human haemoglobin in the visible range, "*Physics in Medicine and Biology* 56, pp 4013-4021.

[23] Schlegel, A., Alvarado, S. F., and Wachter, P., 1979, "Optical Properties of Magnetite (Fe_3O_4), "*Journal of Physics C: Solid State Physics,* vol. 12**,** pp. 1157-1164.

[24] Johnson, P. B., and Christy, R. W., 1972, "Optical Constans of The Noble Metals, "*Phys Rev* B, vol 6**,** No 12.

[25] Chettier, U. K., and Engheta, R., 2012, "Internal homogenization: Effective permittivity of a coated sphere," *Optics Express,* vol. 20, pp**.** 22976-22986.

[26] Rather H 1986 *Surface Plasmons on Smooth and Rough Surfaces and Gratings* Berlin: (Springer-Verlag).

[27] Ghatak, A., and Thyagarajan, K.," *An Introduction to Fiber Optics*" (Cambridge University Press, Cambridge, 1998), pp. 80–82

[28] Le, J., Person, Colas, F., Compere, C., Lehaitre, M. Anne, Boussard-Pledel, C., Bureau, B., Adam, J.,. Deputier, S., and Guilloux-Viry, M., 2008, *Sens.Actuators* B, 130, pp 771.

[29] Wu, W., He, Q., and. Jiang, C, 2008, "Magnetic iron oxide nanoparticles: synthesis and surface functionalization strategies,' Nanoscale Res. Lett, vol 3 pp 397-41.

[30] Gupta, B. D., and Sharma, A. K., 2005, *Sens. Actuators*, B 107, pp 40–45.

[31] Prahl, S. A., 1999, "see http://omlc.ogi.edu/spectra/hemoglobin/index.html for

Optical Absorption of Hemoglobin

[32] Verma, R., Gupta, B. D., and Jha, R., 2011, "Sensitivity enhancement of a surface plasmon resonance-based biomolecules sensor using graphene and silicon layers,' *Sensor and Actuators B: Chemical* 160**,** pp 623-631.